ARTICLES
PUBLISHED ONLINE: 1 FEBRUARY 2016 | DOI: 10.1038/NCHEM.2447
nature chemistry

Chemical amplification of magnetic field effects relevant to avian magnetoreception

Daniel R. Kattnig[1†], Emrys W. Evans[2†], Victoire Déjean[2], Charlotte A. Dodson[3‡], Mark I. Wallace[3], Stuart R. Mackenzie[1], Christiane R. Timmel[2] and P. J. Hore[1*]

Magnetic fields as weak as the Earth's can change the yields of radical pair reactions even though the energies involved are orders of magnitude smaller than the thermal energy, k_BT, at room temperature. Proposed as the source of the light-dependent magnetic compass in migratory birds, the radical pair mechanism is thought to operate in cryptochrome flavoproteins in the retina. Here we demonstrate that the primary magnetic field effect on flavin photoreactions can be amplified chemically by slow radical termination reactions under conditions of continuous photoexcitation. The nature and origin of the amplification are revealed by studies of the intermolecular flavin–tryptophan and flavin–ascorbic acid photocycles and the closely related intramolecular flavin–tryptophan radical pair in cryptochrome. Amplification factors of up to 5.6 were observed for magnetic fields weaker than 1 mT. Substantial chemical amplification could have a significant impact on the viability of a cryptochrome-based magnetic compass sensor.

Among other directional cues, migratory birds use a light-dependent geomagnetic compass for orientation and navigation[1–3]. Although the primary detection mechanism is unclear, the evidence currently points to magnetically sensitive photochemical reactions in cryptochrome proteins located in the retina[4–6]. Cryptochromes[7] contain the chromophore flavin adenine dinucleotide (FAD), photoexcitation of which can trigger three consecutive intraprotein electron transfers along a conserved triad of tryptophan (Trp) residues to produce a ($FAD^{\bullet-}$ $Trp^{\bullet+}$) radical pair[8–10]. This form of cryptochrome is magnetically sensitive *in vitro* and possibly also *in vivo*[11–13]. Similar magnetosensitivity is conceivable in other cryptochrome-derived radical pairs in which $FAD^{\bullet-}$ or its protonated form, $FADH^{\bullet}$, is paired with an ascorbic acid radical[14] or, less plausibly, superoxide, $O_2^{\bullet-}$ (refs 15,16). There appear to be different electron-transfer pathways in some cryptochromes[17,18], but no evidence so far that they give rise to magnetic field effects (MFEs).

The radical pair mechanism is well established as the source of MFEs on chemical reactions[19]. Remarkably, the magnetic interactions of electron spins in organic radicals can result in significant changes in the reaction kinetics and product yields, even though those interactions are many orders of magnitude weaker than the thermal energy, k_BT. The sensitivity to applied magnetic fields derives from the coherent spin dynamics of pairs of radicals formed in spin-correlated states. Several conditions need to be satisfied for a radical pair to be suitable as a geomagnetic compass sensor[5]: (1) the electron spin in at least one of the radicals must interact anisotropically with nuclear spins, (2) the mutual interaction of the two electron spins should be small, (3) the radical pair must react spin selectively, (4) its lifetime should not be too short and (5) the electron-spin relaxation must be relatively slow. Studies of an isolated cryptochrome *in vitro* suggest that the ($FAD^{\bullet-}$ $Trp^{\bullet+}$) radical pair is fit for the purpose of magnetic sensing[11], although the effects of Earth-strength magnetic fields and directional responses have yet to be demonstrated.

Evidence that cryptochromes play a sensory role in magnetoreception is slowly accumulating but still largely circumstantial[6,20,21]. Cryptochromes have been found in the retinas of migratory birds[20,22–24] in various cell types that exhibit neuronal activity when the birds perform magnetic orientation[22]. Behavioural studies of fruit flies suggest that a cryptochrome is required for magnetic sensing[25–31], but do not establish that it is the magnetically sensitive entity. MFEs on blue-light-dependent, cryptochrome-mediated growth responses in plants have been reported[32], but were not replicated in an independent study[33]. Of the known photoreceptors, it appears that only cryptochromes and the closely related photolyases form radical pairs; since their proposal 15 years ago[4], cryptochromes remain the only candidate magnetoreceptor molecules.

Pronounced directional responses of a radical pair reaction to an Earth-strength magnetic field (about 50 μT) at physiological temperatures seem unlikely. Isotropic changes in reaction yields at the 1% level have been reported for a cryptochrome and a photolyase in a 1 mT field[11,34] and theoretical predictions for ($FAD^{\bullet-}$ $Trp^{\bullet+}$) suggest that anisotropic effects at 50 μT might be no larger than 0.1%[14]. Until more is known about the signal-transduction mechanism it is difficult to judge whether such small effects could form the basis of a viable compass[6]. However, it seems reasonable to assume that evolution would have availed itself of any opportunity to boost the sensitivity of the fundamental response so as to optimize the compass. One theoretical possibility (for which there is currently no biological evidence) is that the magnetic field experienced by a radical pair sensor could be amplified by nearby magnetic nanoparticles composed of biogenic magnetite[35–37].

We present here experimental evidence for a chemical amplification mechanism in which slow reaction steps in the cryptochrome photocycle can significantly boost the response to a weak magnetic field. These enhancements, which have not been observed previously, were found for continuous illumination under conditions that allow long-lived reaction intermediates to accumulate. The details of the amplification process were characterized through

[1]Department of Chemistry, University of Oxford, Physical & Theoretical Chemistry Laboratory, Oxford OX1 3QZ, UK. [2]Department of Chemistry, University of Oxford, Inorganic Chemistry Laboratory, Oxford OX1 3QR, UK. [3]Department of Chemistry, University of Oxford, Chemistry Research Laboratory, Oxford OX1 3TA, UK. †These authors contributed equally. ‡Present address: Molecular Medicine, National Heart & Lung Institute, Imperial College London, London SW7 2AZ, UK. *e-mail: peter.hore@chem.ox.ac.uk

studies of intermolecular photoreactions of flavins and the photo-induced intramolecular radical pair ($FAD^{\bullet-}$ $Trp^{\bullet+}$) in cryptochrome. We end by arguing that if such amplification occurred in a cryptochrome-based sensor *in vivo*, the detection sensitivity could be boosted by more than an order of magnitude.

Results and discussion

MFEs on intermolecular flavin photocycles. MFEs on flavin (F) photochemistry are generally well understood (Fig. 1)[38–43]. Photoexcitation of the fully oxidized state ($F \rightarrow {}^1F^*$) is followed either by fluorescence (${}^1F^* \rightarrow F$) or intersystem crossing (${}^1F^* \rightarrow {}^3F^*$). Intermolecular electron transfer from a closed-shell electron donor, D, to the triplet flavin gives a triplet radical pair, ${}^3(F^{\bullet-}\ D^{\bullet+})$, which interconverts coherently with the corresponding singlet state, ${}^1(F^{\bullet-}\ D^{\bullet+})$ (curly arrows in Fig. 1). At the same time, (1) a reverse electron transfer returns ${}^1(F^{\bullet-}\ D^{\bullet+})$ to the ground-state reactants and (2) $F^{\bullet-}$ and $D^{\bullet+}$ diffuse apart to form independent free radicals. Bulk re-encounter of $F^{\bullet-}$ and $D^{\bullet+}$ regenerates ${}^1(F^{\bullet-}\ D^{\bullet+})$ and ${}^3(F^{\bullet-}\ D^{\bullet+})$ in the statistical ratio of 1:3. In the absence of strong heavy-atom-mediated spin–orbit interactions all the electron-transfer steps conserve electron spin. The reaction steps labelled k_F and k_D in Fig. 1 are discussed below.

The sensitivity to applied magnetic fields lies in the conversion of ${}^3(F^{\bullet-}\ D^{\bullet+})$ into ${}^1(F^{\bullet-}\ D^{\bullet+})$, which is driven by the magnetic (hyperfine) interactions of the electron spins with the spins of magnetic nuclei (^1H and ^{14}N) and by the (Zeeman) interaction of the electron spins with applied magnetic fields. A magnetic field stronger than the hyperfine interactions (~3 mT) energetically isolates two of the three triplet sublevels, which inhibits triplet → singlet conversion and therefore reduces the fraction of radical pairs that returns directly to the ground-state reactants. Reported MFEs[38–40] and other spin-dependent phenomena[44–46] are consistent with Fig. 1.

Under conditions of continuous low-intensity photoexcitation, only the free radicals and the ground-state reactants have appreciable concentrations. The other species have lifetimes of less than a microsecond and are consequently present at much lower photostationary levels (Supplementary Section C). When a strong magnetic field is switched on, and the return of radical pairs to the ground state becomes less efficient, the photocycle re-equilibrates to a state in which there are more free radicals and correspondingly fewer ground-state molecules. Consequently, there is a reduction in the fluorescence of ${}^1F^*$ whose concentration is proportional to that of the ground state (F).

Flavin–lysozyme MFEs. Initial experiments were conducted using intermolecular models of the intramolecular flavin–Trp radical pair in a cryptochrome. Hen-egg white lysozyme (a 14 kD protein) was chosen as the electron donor because it is known to form radical pairs ($F^{\bullet-}\ D^{\bullet+}$), in accord with Fig. 1, by electron transfer from a solvent-exposed Trp residue on the surface of the protein to photoexcited triplet states of flavins[30,31]. Fluorescence-detected MFEs for this photoreaction are shown in Fig. 2. An aqueous solution of flavin mononucleotide (FMN) and lysozyme was irradiated continuously with a 470 nm laser for a period of several minutes, with the fluorescence monitored continuously. Throughout the measurement a magnetic field was switched between 0 and 27 mT every 1.68 seconds. Superimposed on a gradual (tens of seconds) decrease in the fluorescence intensity (Fig. 2a) (which we attribute to a combination of re-equilibration of the photocycle, photobleaching reactions and diffusion) is a small but distinct modulation in synchrony with the magnetic field steps. As the background fluorescence intensity drops, so does the amplitude of the field-induced modulations. That is, the relative change in the fluorescence does not change significantly with time. Figure 2b shows this variation averaged over a large number of field cycles. The data are presented as the fractional

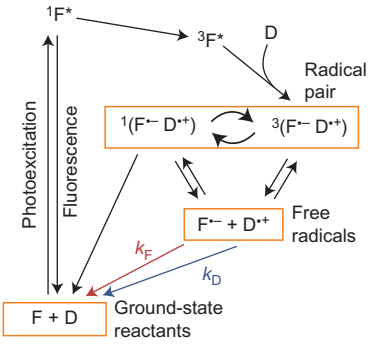

Figure 1 | Intermolecular radical pair reactions of flavins. Reaction scheme for the intermolecular photochemical reaction of a flavin (F) with an electron donor (D). The radicals, $F^{\bullet-}$ and $D^{\bullet+}$, are either charged as shown or (de)protonated depending on the pH. The slow reaction steps labelled with the rate constants k_D and k_F are responsible for the amplification of the MFE. The other reaction steps are as follows: photoexcitation of the ground-state flavin (F) to its first excited singlet state (${}^1F^*$); fluorescence of ${}^1F^*$; intersystem crossing from ${}^1F^*$ to the excited triplet state of the flavin (${}^3F^*$); spin-conserving electron transfer from the donor D to ${}^3F^*$ to form the triplet state of the radical pair, ${}^3(F^{\bullet-}\ D^{\bullet+})$; coherent interconversion of the triplet and singlet, ${}^1(F^{\bullet-}\ D^{\bullet+})$, radical pair states driven by hyperfine and Zeeman magnetic interactions (curly arrows); spin-allowed reverse electron transfer within the singlet radical pair, which regenerates the ground state of both reactants; diffusive separation to form free radicals, which subsequently re-encounter to form radical pairs. Singlet–triplet interconversion becomes less efficient in a magnetic field stronger than the hyperfine interactions because only the T_0 triplet substate is able to mix with the singlet, whereas T_{+1} and T_{-1}, as well as T_0, mix with the singlet when the external magnetic field is weaker than the hyperfine interactions.

change in the intensity of the fluorescence relative to the field-off condition. As anticipated, switching the field on/off caused a reduction/increase in the fluorescence. Although the changes are relatively small, the signal-to-noise is excellent and the signals were highly reproducible.

Remarkably, the MFE in Fig. 2b shows biphasic kinetics. After switching the field on, a fast component (<1 ms) was followed by a much slower phase with an exponential time constant of $\tau = 470 \pm 10$ ms. The same pattern of fast and slow phases was seen when the field was switched off. The amplitudes of the two components were used to define prompt (χ_P) and delayed (χ_d) MFEs (Fig. 2b). The amplification factor, E, defined as χ_d/χ_P, was 2.320 ± 0.007. The fast component immediately after the field jump is attributed to the attainment of a new steady state at a rate limited by the bulk re-encounter of the free radicals $F^{\bullet-}$ and $D^{\bullet+}$. The timescale of this process is estimated at 0.2–1.0 ms, based on a diffusion-controlled rate constant (~10^9 M^{-1} s^{-1}) and 1.0–5.0 μM concentrations of $F^{\bullet-}$ and $D^{\bullet+}$. The slow components in Fig. 2b were unexpected.

Flavin–Trp MFEs. To see whether the MFEs observed for FMN reacting with lysozyme were influenced by the electron donor being part of a large (protein) molecule, we studied the same photoreaction, but with the tryptophan present as the free amino acid. Figure 1 should still be appropriate, but with different rate constants for some of the reaction steps. Similar biphasic kinetics were observed (Fig. 2d,e) except that the slow component of the fluorescence had the opposite phase, that is, $\chi_d < \chi_P$ ($E = 0.644 \pm 0.003$), and was an order of magnitude faster ($\tau = 55 \pm 1$ ms) than for the Trp residues in lysozyme. For both the FMN/lysozyme and FMN/Trp reactions there was no statistically significant difference between individual cycles (Fig. 2a,d) and their means (Fig. 2b,e, respectively). In both cases, the averaged responses to switching

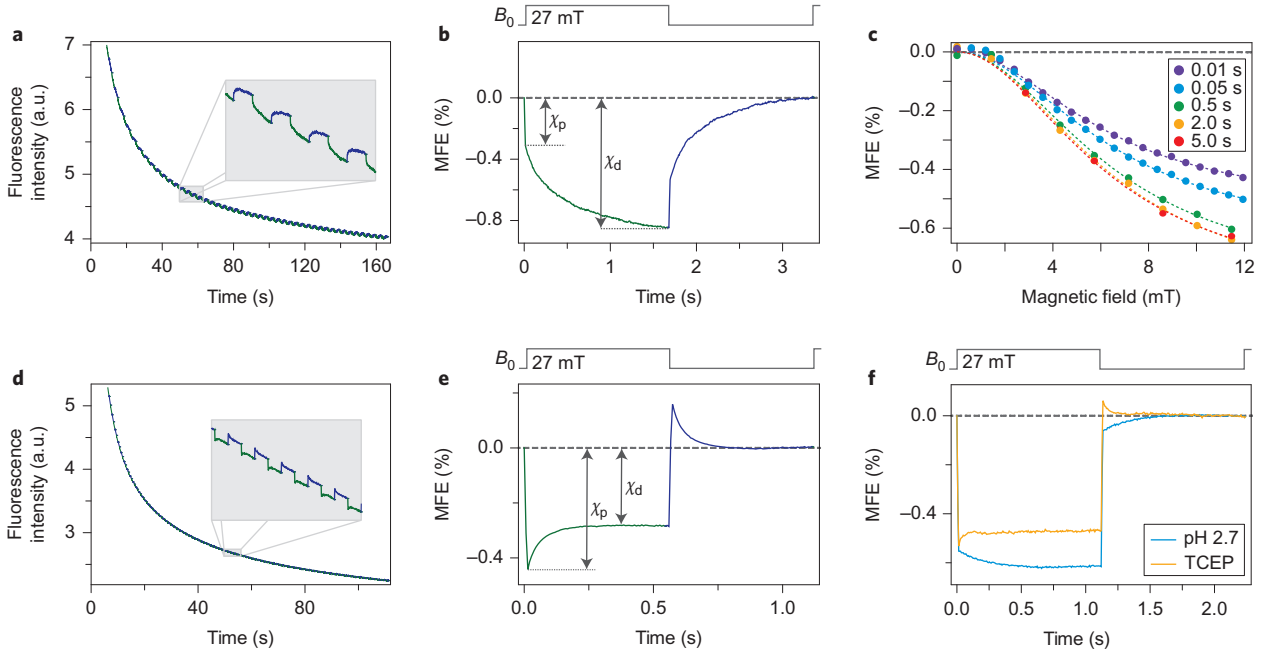

Figure 2 | Amplified MFEs in intermolecular reactions of flavins. a, Fluorescence intensity of an aqueous solution (pH 4.0) of FMN (10 μM) and lysozyme (0.5 mM) as a function of the time after the onset of continuous illumination (470 nm) with an applied magnetic field switched between 0 and 27 mT every 1.68 seconds. Modulation of the fluorescence intensity, shown expanded in the inset, occurs in synchrony with the magnetic field switching. **b**, The average of the responses in **a** to one cycle of the magnetic field shows a prompt MFE (χ_p) and a slowly established delayed MFE (χ_d). **c**, Dependence of the MFE on the magnetic field strength for different delay times between switching the field on and measuring the fluorescence. The dashed lines are Lorentzian fits to the data used to determine the $B_{1/2}$ values. **d**, As **a**, but for a solution (pH 6.2) of FMN (10 μM) and Trp (1.0 mM). The magnetic field was switched between 0 and 27 mT every 0.56 seconds. **e**, Average of the responses in **d** to one cycle of the magnetic field. In contrast to **b**, the delayed MFE (χ_d) is smaller than the prompt effect (χ_p). **f**, As **e**, but with the pH reduced to 2.7 (citric acid buffer) (blue) and with 50 μM TCEP (pH 6.2) (orange), which shows that the amplification factor can be changed by altering the rate constants k_D and k_F. The data in the field-on and field-off periods in **a**, **b**, **d** and **e** are shown in green and blue, respectively. The timing of the magnetic field steps is shown in grey at the top of **b**, **e** and **f** (B_0 is the magnetic field strength). In **b** and **e**, the slow background decay of the fluorescence (visible in **a** and **d**) has been subtracted.

the field on and off had identical amplitudes and kinetics within experimental error.

Dependence on magnetic field intensity. A clue to the origin of the slow phase comes from the dependence of its amplitude on the strength of the applied magnetic field. Figure 2c shows the fluorescence-detected MFE for the FMN/lysozyme reaction measured at different times (T = 10–5,000 ms) after the field was switched on (see Methods and Supplementary Sections A and B for the experimental details). As expected from Fig. 2b, the MFE became more negative with increasing T. The field, $B_{1/2}$, at which it reached 50% of its limiting value (obtained by Lorentzian fitting and extrapolation) was 6.4 ± 0.2 mT. This number, which was found to be independent of T, is consistent with the hyperfine interactions in the flavin–Trp radical pair augmented by a contribution from electron-spin relaxation[11,40]. The invariance of $B_{1/2}$ indicates that no other mechanisms, for example, triplet–triplet or triplet–doublet pairs[47,48], are involved. The wavelength dependence of the fluorescence (Supplementary Section B) is consistent with ^{1}FMN* being the sole source of both fast and slow components.

Slow radical termination reactions. The reaction scheme, as discussed above, cannot account for the slow phase in Fig. 2b,e. Simulations that used independently determined values of the rate constants of the various steps in the photocycle (Supplementary Section C) show that the fluorescence-detected MFE should be monophasic with a short time constant (about 100 μs) determined by the bulk re-encounter of $F^{\bullet-}$ and $D^{\bullet+}$. However, biphasic kinetics can be obtained by introducing additional slow reaction steps that return the free radicals to their respective ground states (coloured arrows in Fig. 1). For simplicity, these reactions, with rate constants k_F and k_D, are assumed to have first-order kinetics. When $k_F = k_D$, the extra pathways do not affect the simulated kinetics, which remain fast (~100 μs (Fig. 3a left)). However, when $k_F \neq k_D$, the prompt effect is followed by a slow phase. If $k_D/k_F > 1$, the MFE is enhanced ($E > 1$ (Fig. 3a, right)); if $k_D/k_F < 1$, the MFE is attenuated ($E < 1$ (Fig. 3a, centre)). In both cases, the timescale of the slow component is determined by the values of k_F and k_D.

For a broad range of values of the two rate constants, E was found to depend principally on the ratio k_D/k_F (Fig. 3b). Surprisingly large steady-state enhancements can result from these very slow processes. For k_D and k_F in the range of 10^{-1} to 10^3 s^{-1}, amplification factors of 5–20 can be realized using independently determined or estimated values for the other rate constants in the reaction scheme (Supplementary Section C). Lower light intensities were found to lead to larger enhancements (Supplementary Section C).

Rate constants. Incorporation of the additional radical termination reactions into the photocycle also allowed a quantitative analysis of the kinetics in Fig. 2b,e (Supplementary Section C). For the FMN/lysozyme case, we find $k_F = 0.70$ s^{-1} and $k_D = 4.9$ s^{-1}; and for FMN/Trp, $k_F = 70$ s^{-1} and $k_D = 12$ s^{-1}. An approximate treatment of the kinetics (using a highly simplified version of the intermolecular reaction scheme (Supplementary Section D)) suggests that $E \approx \sqrt{(k_D/k_F)}$. For these two reactions $\sqrt{(k_D/k_F)} = 2.6$ and 0.41, respectively, which agree reasonably well with the experimental amplification factors, $E = 2.320$ and 0.644, respectively, as reported above.

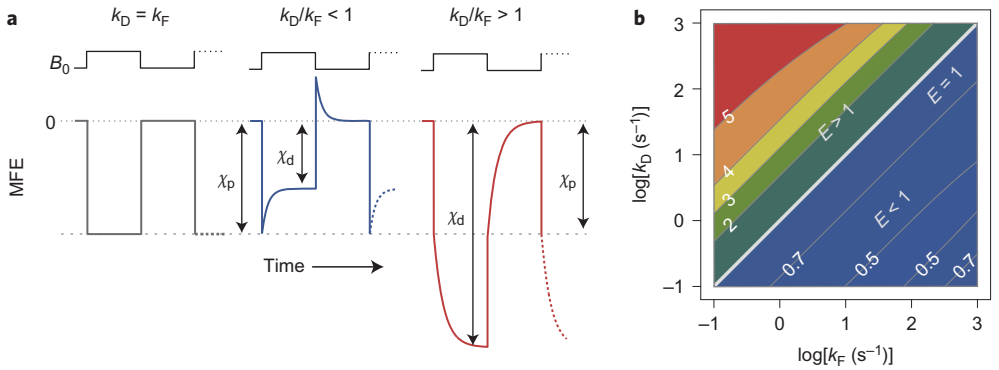

Figure 3 | Characteristics of the amplified MFE. a, Response of the concentration of the flavin excited state, $^1F^*$, to sudden on/off switching of an external magnetic field (B_0). Left, $k_F = k_D$ ($E = 1$); centre, $k_D/k_F < 1$ ($E < 1$); right, $k_D/k_F > 1$ ($E > 1$). Depending on the ratio of their rate constants, k_D/k_F, the radical termination reactions lead to a slow kinetic phase that enhances or attenuates the prompt MFE. **b**, Contour plot of the amplification factor, E, as a function of the slow radical termination rate constants k_F and k_D. E depends principally on the ratio k_D/k_F; the largest amplification factors occur when $k_D >> k_F$. The simulations were performed for an initial triplet radical pair and a strong magnetic field. The values of the other rate constants used in the simulation are given in Supplementary Section C.

The smaller value of k_D for the lysozyme reaction presumably arises from the lower accessibility of the Trp residues in the protein compared with that of the free amino acid[49]. The values of k_F for the two reactions can be understood as follows. The $FMNH^\bullet$ radical has a pK_a of 8.6 (refs 50,51) so that there is a higher fraction of $FMN^{\bullet-}$ present in the Trp experiment (pH 6.2) than in the lysozyme case (pH 4.0). A likely contributor to the flavin radical termination reaction is oxidation by molecular oxygen, which is 10^3–10^4 times faster for $FMN^{\bullet-}$ than for $FMNH^\bullet$ (refs 50,51). Removal of flavin radicals should therefore be slower at a lower pH. In accord with this, reducing the pH of the FMN/Trp reaction from 6.2 to 2.7 changes the amplification factor from $E < 1$ (Fig. 2e) to $E > 1$ (Fig. 2f), consistent with a substantial reduction in k_F.

Further observations. Further support for the importance of slow radical termination reactions comes from three additional observations made by changing the experimental conditions in ways that were expected to alter the ratio of k_D to k_F. First, the addition of 50 μM of the reductant tris(2-carboxyethyl)phosphine (TCEP) to the FMN/Trp reaction at pH 6.2 increased E from 0.644 (Fig. 2e) to 0.89 ± 0.02 (Fig. 2f) by increasing the rate of reduction of the Trp radical (k_D). Second, the presence of 20% glycerol boosted E for the FMN/lysozyme reaction from 2.32 (Fig. 2b) to 3.55 ± 0.02 and changed τ from 470 to 2,200 ms (Supplementary Section B). The increase in solvent viscosity presumably reduces the diffusion-controlled contributions to k_D and k_F in such a way that k_D/k_F becomes larger. Third, increasing either the concentration of FMN or the light intensity resulted in a reduction in E for the FMN/Trp reaction, which implies a decrease in k_D/k_F. Both observations may be understood by considering the probable mechanisms of the $FH^\bullet \rightarrow F$ oxidation step. One route for the removal of flavin radicals is disproportionation ($2FH^\bullet \rightarrow F + FH_2$ (refs 50,51)). Another involves molecular oxygen ($FH^\bullet + O_2 \rightarrow F + O_2^{\bullet-} + H^+$, followed by the much faster reaction, $FH^\bullet + O_2^{\bullet-} + H^+ \rightarrow F + H_2O_2$ (refs 50,51)). Both processes result in a supralinear dependence of the oxidation rate constant (k_F) on the flavin radical concentration because of the second-order kinetics of the first and the autocatalytic nature of the second. The involvement of oxygen was confirmed by the observation of an increase in the amplification factor for deoxygenated solutions, consistent with an increase in k_D/k_F (Supplementary Section E).

Origin of the amplification. The origin of the enhanced MFE when $k_D > k_F$ (Fig. 2b and the right-hand side of Fig. 3a) may be understood as follows. When the magnetic field is switched on, the fluorescence initially decreases because of the increase in the concentration of free radicals, as explained above. On the completion of this rapid (submillisecond) phase, the concentrations of the free radicals ($F^{\bullet-}$ and $D^{\bullet+}$ in Fig. 1) are equal. Then, as the k_F and k_D steps start to take effect (>10 ms), the faster removal of $D^{\bullet+}$ (when $k_D > k_F$) causes its concentration to drop more rapidly than that of $F^{\bullet-}$. Consequently, the lifetime, and therefore the steady-state concentration of $F^{\bullet-}$, increases, the concentration of ground-state flavin falls and, therefore, so does the fluorescence intensity. The opposite change occurs when $k_D < k_F$. The slow termination steps have a negligible effect on the magnetic sensitivity when measured under flash-photolysis conditions because they cannot compete with the much faster radical–radical recombination reaction. This explanation of the amplification effect was corroborated by experiments using square-wave-modulated light intensities, in the absence of a magnetic field, as an alternative way to shift the position of the photostationary state (Supplementary Section F).

Flavin–ascorbic acid MFEs. Next, we explored the amplification for the photoreaction of FMN with ascorbic acid. This electron donor was chosen because the radical pair it forms with FMN is expected to be considerably more sensitive to weak magnetic fields than ($FMN^{\bullet-}$ $Trp^{\bullet+}$) by virtue of the much smaller hyperfine interactions in the ascorbyl radical[14]. The magnetic field dependence of the fluorescence (Fig. 4a), recorded in the same manner as that in Fig. 2c, showed the biphasic behaviour that is typical of long-lived radical pairs. The positive MFE, with a peak intensity at approximately 0.7 mT and a zero crossing close to 1.4 mT, is known as the 'low field effect'[52,53].

Figure 4b,c shows averaged fluorescence-detected MFEs for the FMN/ascorbic acid reaction with the field cycled between 0 and 27 mT and between 0 and 0.7 mT, respectively. As expected from Fig. 4a, the latter is weaker than the former and of opposite phase. Less predictably, the amplification factor is larger for the weaker field, $E = 1.98 \pm 0.02$ at 27 mT and 5.6 ± 0.3 at 0.7 mT. The kinetics of the slow phase are also a little different, $\tau = 170$ ms at 27 mT and 190 ms at 0.7 mT. The origin of both differences may again be understood in terms of the supralinear nature of the slow processes that oxidize $FH^\bullet$. The prompt MFE at 27 mT (0.7 mT) leads to an increase (decrease) in the $FH^\bullet$ concentration and a disproportionate increase (decrease) in k_F. This translates into a larger E and a longer τ at 0.7 mT.

Cryptochrome photocycle. We now turn from bimolecular electron-transfer reactions to the intramolecular photochemistry

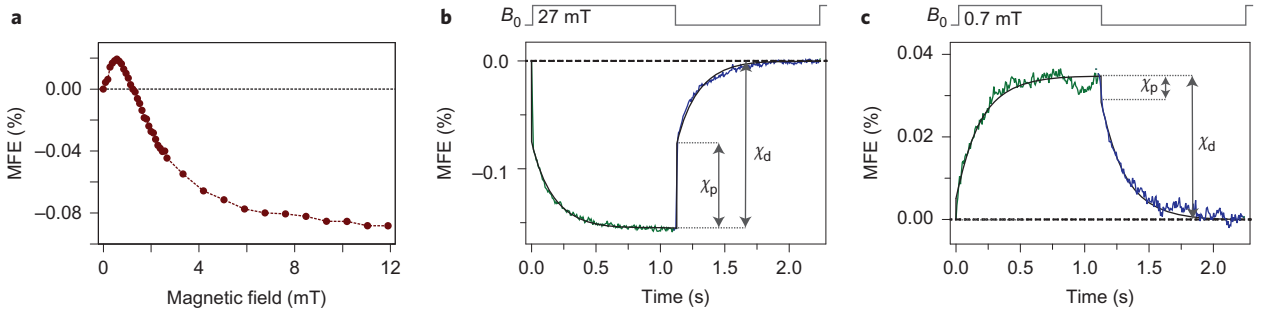

Figure 4 | Amplified MFEs in the low-field region. a, Dependence of the MFE on the magnetic field strength for an aqueous solution (pH 3.8) of FMN (10 μM) and ascorbic acid (0.5 mM) with a 50 ms delay time between switching the field on and measuring the fluorescence. The positive MFE at fields below 1.4 mT is known as the low field effect; it is particularly prominent in this case because of the small hyperfine interactions in the ascorbyl radical. **b**, Average of the responses to one cycle of a magnetic field switched between 0 and 27 mT every 1.12 seconds. **c**, As **b**, but for a 0.7 mT magnetic field (in the region of the low field effect). The prompt and delayed components have opposite phases in **b** and **c** because of the biphasic form of the MFE (shown in **a**). The black lines in **b** and **c** are fits to single exponentials.

of cryptochromes (Fig. 5). Photoexcitation of the fully oxidized state of the FAD cofactor leads to a ($FAD^{\bullet-}$ $Trp^{\bullet+}$) radical pair (termed RP1 in Maeda *et al.*[11]) in which $Trp^{\bullet+}$ is the oxidized form of the terminal residue of the Trp-triad electron-transfer chain. One difference from the reactions shown in Fig. 1 is that the intraprotein electron transfer is markedly faster than the intersystem crossing ($^1FAD^* \rightarrow {}^3FAD^*$) and produces the radical pair in an initial singlet state[11,34,54]. The singlet state of the radical pair either undergoes a reverse electron transfer to regenerate the ground states of the flavin and the Trp or is converted coherently into the triplet radical pair state. However, there the correspondence with Fig. 1 ends. Instead of a diffusive separation of the radicals (impossible in the protein), one or both of $FAD^{\bullet-}$ and $Trp^{\bullet+}$ changes its protonation state to give a longer-lived, magnetically insensitive radical pair (denoted RP2 in Maeda *et al.*[11]). The constituents of RP2 are then independently returned to their respective ground states by slow redox reactions analogous to the k_F and k_D processes illustrated in Fig. 1. Despite the differences in the two reaction schemes, amplification of the MFE ($E > 1$) is expected for the intramolecular photocycle provided $k_D > k_F$ (Supplementary Sections C and D).

Cryptochrome MFEs. Figure 6a shows the difference between the fluorescence spectra of *Arabidopsis thaliana* cryptochrome (*At*Cry1) with and without a 12.2 mT magnetic field. The signal

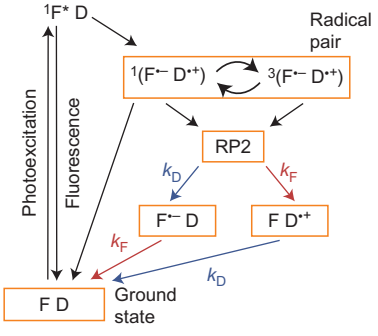

Figure 5 | Intramolecular radical pair reactions of cryptochromes. Reaction scheme for the intramolecular photochemistry of the FAD (F) and the terminal residue of the Trp triad in cryptochrome as the electron donor (D). RP2 is a FAD–Trp radical pair in which the flavin radical ($F^{\bullet-}$) is protonated or the Trp radical ($D^{\bullet+}$) is deprotonated or both; it is not magnetically sensitive. The slow steps labelled with the rate constants k_D and k_F are responsible for the amplification of the MFE. As shown, we assume that the flavin radical may be oxidized before or after the Trp radical is reduced.

grew dramatically in strength as the delay, T, between applying the field and recording the fluorescence was increased from 0.5 to 3.5 seconds. All such spectra closely matched the fluorescence spectrum recorded without an applied field, which demonstrates that the only magnetically sensitive luminescent state is $^1FAD^*$. Changes in the time dependence of the fluorescence produced by magnetic field cycling are shown in Fig. 6b. These signals are much weaker than those for the intermolecular reactions (above) for two main reasons. First, the picosecond electron transfer in the cryptochrome results in a low fluorescence quantum yield[55,56]. Second, the k_F and k_D steps are much slower than those for the FMN reactions (Figs. 2 and 4), which means that even with the low light intensities used for these measurements there is a substantial depletion of the ground state and hence a reduction in the fluorescence intensity. Figure 6b shows an enhanced MFE growing in over several seconds ($\tau = 3.4 \pm 0.9$ s). The addition of 50 μM TCEP to accelerate the reduction of the $Trp^{\bullet+}$ radical (Fig. 6c) boosted the signal and caused it to rise more rapidly ($\tau = 1.7 \pm 0.1$ s). In addition, a small prompt MFE was present (in Fig. 6c more clearly than in Fig. 6b).

We attribute the slow components in Fig. 6b,c to the radical termination steps in the cryptochrome with $k_D > k_F$, as for the FMN/lysozyme reaction (Fig. 2b), but with the opposite phase to FMN/lysozyme because the initial state of the radical pair in the protein is singlet rather than triplet. The small prompt MFE is assigned to the photoreaction of a small amount of free FAD with Trp residues on the surface of the protein[44]. This signal, which (as expected) has the same phase as that of the prompt MFE seen for the FMN/lysozyme reaction, obscures any prompt MFE from the cryptochrome. There is no evidence that free FAD leads to an intermolecular delayed MFE—any such effect would occur with faster kinetics than seen in Fig. 6b. A kinetic analysis of the cryptochrome photocycle in Fig. 5 (Supplementary Sections C and D) shows that substantially enhanced MFEs can be anticipated when $k_D > k_F$.

Cryptochrome magnetic signalling. The data in Fig. 6a–c demonstrate a substantial amplification of the MFE on the cryptochrome photocycle, using FAD fluorescence as a direct indicator of the concentration of the ground state of the protein. To relate these findings to the putative role of cryptochromes in the avian magnetic compass, it is important to establish whether there is also an amplification effect on the signalling state of the protein. Although almost nothing is known about magnetic signal transduction by cryptochromes, it seems improbable that the ground state of the protein is responsible. We presume that the magnetically sensitive radical pair state (~1 μs lifetime[11]) leads to a longer lived species—for example, the stabilized radical pair

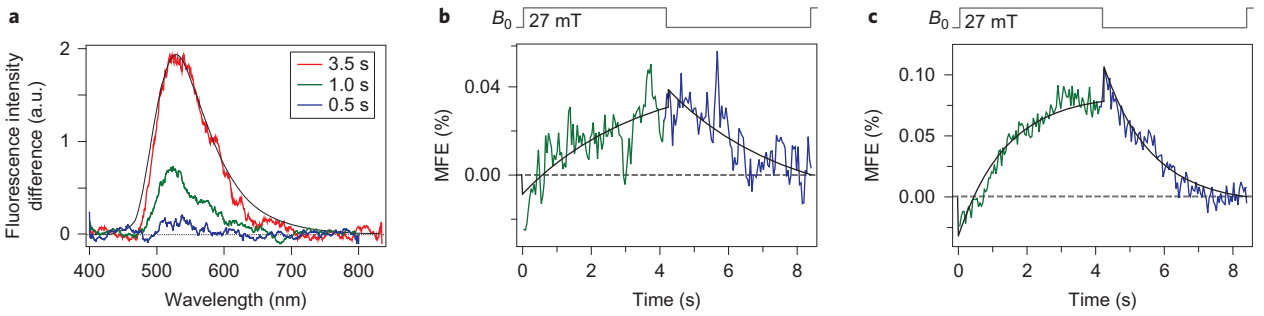

Figure 6 | Amplified MFEs in a cryptochrome. a, Changes in the fluorescence spectrum of an aqueous solution of *At*Cry1 (about 100 μM, 10 mM Tris, pH 7.4, 150 mM NaCl, 30% glycerol v/v) induced by a magnetic field. Spectra (smoothed using a 25 nm moving average filter) are shown for different delay times, *T*, after switching on a 12.2 mT magnetic field, having subtracted the zero-field spectrum. The MFE becomes dramatically stronger as *T* is increased from 0.5 to 3.5 seconds. The black trace is the fluorescence spectrum measured in the absence of a magnetic field and scaled to match the maximum of the difference spectrum at $T = 3.5$ seconds (red trace). **b**, Average of the responses of an aqueous solution of *At*Cry1 (about 100 μM, pH 7.4) to one cycle of a magnetic field switched between 0 and 27 mT every 4.2 seconds. The enhanced MFE grows over a period of several seconds as a result of the slow radical termination reactions ($k_D > k_F$). **c**, As **b** but with the addition of TCEP (50 μM). An accelerated reduction of the $Trp^{\bullet+}$ radical by the TCEP boosts the MFE ($k_D >> k_F$) and causes it to grow more rapidly. In **b** and **c** the black lines are fits of the data to single exponentials assuming symmetric responses to switching the field on and off.

state RP2 characterized by Maeda *et al.* (~100 μs lifetime)[11]—which could, in turn, give rise to a signalling state. It seems plausible that the latter would be stabilized further against a reverse electron transfer by reduction of the Trp radical by an exogenous electron donor. In terms of the reactions studied here, this situation corresponds to $k_D > k_F$ and therefore an amplification factor $E > 1$. The question is therefore whether the MFE on the radical form of the protein is amplified by the asymmetry in the slow radical termination reactions.

Although we present relative (percentage) MFEs in Figs 2, 4 and 6, this is probably not the relevant quantity for magnetic signalling: even a large relative change in the steady-state concentration of the signalling state is unlikely to form the basis of a magnetic compass if that concentration is tiny. The quantity that determines the signal-to-noise ratio of the sensor is more likely to be the absolute change in the concentration of the radicals present under steady-state conditions. This is the basis of the analysis of magnetoreceptor sensitivity by Weaver *et al.*[57], who considered the change in the absolute number of neurotransmitter molecules supposedly formed from the radical pair state. We therefore calculated the prompt and steady-state changes in the concentration of the FAD-radical form of the protein as a function of k_D and k_F using the reaction scheme in Fig. 5 and a kinetic analysis described in Supplementary Section C. The results are shown in Fig. 7. The largest delayed (steady-state) field-induced concentration changes occur when $k_D >> k_F$ and are substantially larger than the prompt effect for any values of k_D and k_F. Furthermore, when the light intensity is reduced, a larger ratio of k_D/k_F is necessary to achieve a significant amplification (Supplementary Section C). That is, the lower the light intensity, the more important is the amplification phenomenon.

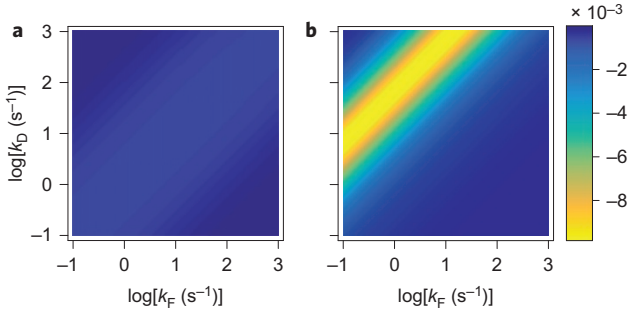

Figure 7 | Simulations of changes in radical concentrations induced by a magnetic field. a, Density plot of the absolute prompt change in the total concentration of flavin radicals produced by an applied magnetic field, plotted as a function of the radical termination rate constants k_F and k_D. **b**, As **a**, but showing the absolute steady-state change induced by a magnetic field. The scale bar refers to both plots. The amplification factor in the centre of the yellow region of **b**, where the absolute steady-state change is largest, has a value of 33.

Conclusions

Slow radical termination reactions have been shown to lead to a significant amplification of the effects of weak magnetic fields on flavin-containing radical pairs under conditions of continuous photoexcitation. That these enhancements have not previously come to light is probably because most studies were either conducted with pulsed illumination[11,58] or used magnetic fields that were amplitude modulated at frequencies faster than the slow reaction steps[59]. The magnitude of the amplification increases with the ratio k_D/k_F of the rate constants for the oxidation of the flavin radical, k_F, and the reduction of the counter radical, k_D. Significant amplification factors, *E*, have been observed for cryptochromes and the related intermolecular photochemistry of free flavin molecules. The amplification factors are larger in weaker fields.

We see no obvious reason why the chemical amplification mechanism studied here could not function in a cryptochrome magnetoreceptor. *In vivo* photoexcitation of cryptochromes leads to the accumulation of states of the protein that contain reduced forms of FAD[60], which implies an efficient reduction of the donor radical and hence substantial enhancement of the MFE (that is, $k_D >> k_F$ and hence $E >> 1$). It has been suggested that the signalling state of the putative cryptochrome magnetosensor contains FAD that is either singly reduced ($FAD^{\bullet-}$ or $FADH^{\bullet}$)[61] or, after further photoexcitation, fully reduced ($FADH^-$)[12,13]. Either way, a rapid reduction of the donor radical would stabilize the signalling state against reverse electron transfer and so promote signal transduction. There appears to be ample scope for evolution to have optimized the amplification by tuning k_D and k_F via factors such as the redox potentials of the flavin and donor radicals and their accessibility to, and the local concentrations of, intracellular oxidants and reductants. We suggest that substantial chemical amplification of radical pair MFEs could have a significant impact on the viability of a cryptochrome-based magnetic compass sensor.

Methods

Spectrally resolved fluorescence measurements. Square-wave-modulated magnetic fields of up to 12 mT (rise time 3 ms) were generated using Helmholtz coils (diameter 3.6 cm). Samples positioned between the coils were irradiated with one of two continuous-wave diode lasers (405 and 450 nm); where appropriate, the excitation power was attenuated by neutral density filters. Fluorescence was dispersed by a spectrograph onto a charge-coupled device (CCD) camera in which the fluorescence was integrated for a period of 20–500 ms following a set delay, *T*, after switching on the field. For each magnetic field strength, 35–900 measurements were averaged in a randomized order. Experiments were conducted at the following laser powers, laser wavelengths and sample temperatures: 270 mW, 405 nm, 22 °C (Fig. 2c); 350 mW, 405 nm, 22 °C (Fig. 4a); and 1 mW, 450 nm, 5 °C (Fig. 6a).

Time-resolved fluorescence measurements. The data shown in Figs 2a,b,d–f, 4b,c and 6b,c were acquired using an inverted fluorescence microscope. Samples (optical path length 0.5 mm, depth of field 0.8 μm) were epi-illuminated with the attenuated and expanded beam of a 470 nm, 80 mW diode laser focused at the back aperture of an oil-immersion objective. The fluorescence was collected through the same objective and recorded using an electron-multiplying CCD camera. Magnetic fields (up to 27 mT, < 70 μs rise time) were generated by a solenoid wound around a ferrite core (diameter 3 mm) fixed in a non-metallic mount along the optical axis and placed 1 mm above the sample. For the results in Figs 2 and 4, the camera exposure time was 5 ms per frame and the interval between frames was 7 ms. Typically, 16,000 frames were recorded with the field stepped between zero and a preset value every 80, 160 or 240 frames. For the data in Fig. 6, 10, 000 frames were recorded with a camera exposure time of 40 ms per frame and a frame interval of 42 ms, with the field switched every 100 frames. For the cryptochrome measurements, the diode laser output was highly attenuated (to 0.1 mW) and the stage cooled to −5 °C (sample temperature approximately 2 °C) to minimize sample photodegradation. All the other measurements were performed at 22 °C.

Sample preparation. *At*Cry1 was expressed in *Nicotiana benthamiana* (Planet Biotechnology). All studies were conducted on freshly defrosted samples. During the final sample preparation and purification step, protein solutions were shielded from ambient light and kept at temperatures below 4 C. For the fluorescence measurements, *At*Cry1 (about 100 M) was contained in 10 mM Tris, 0.15 mM NaCl, 30% glycerol v/v, pH 7.4. The concentration of the flavin was verified spectrophotometrically.

Modelling amplification effects. Details of the simulation methods, both for inter- and intramolecular flavin-containing radical pairs, are described in Supplementary Sections C and D.

Received 17 July 2015; accepted 18 December 2015; published online 1 February 2016

References

1. Wiltschko, R. & Wiltschko, W. Avian magnetic compass: its functional properties and physical basis. *Curr. Zool.* **56,** 265–276 (2010).
2. Mouritsen, H. in *Neurosciences—from Molecule to Behavior: a University Textbook* (eds Galizia, C. G. & Lledo, P.-M.) 427–443 (Springer-Verlag, 2013).
3. Kishkinev, D. A. & Chernetsov, N. S. Magnetoreception systems in birds: a review of current research. *Biol. Bull. Rev.* **5,** 46–62 (2015).
4. Ritz, T., Adem, S. & Schulten, K. A model for photoreceptor-based magnetoreception in birds. *Biophys. J.* **78,** 707–718 (2000).
5. Rodgers, C. T. & Hore, P. J. Chemical magnetoreception in birds: a radical pair mechanism. *Proc. Natl Acad. Sci. USA* **106,** 353–360 (2009).
6. Mouritsen, H. & Hore, P. J. The magnetic retina: light-dependent and trigeminal magnetoreception in migratory birds. *Curr. Opin. Neurobiol.* **22,** 343–352 (2012).
7. Chaves, I. *et al.* The cryptochromes: blue light photoreceptors in plants and animals. *Annu. Rev. Plant Biol.* **62,** 335–364 (2011).
8. Giovani, B., Byrdin, M., Ahmad, M. & Brettel, K. Light-induced electron transfer in a cryptochrome blue-light photoreceptor. *Nature Struct. Biol.* **10,** 489–490 (2003).
9. Zeugner, A. *et al.* Light-induced electron transfer in *Arabidopsis* cryptochrome-1 correlates with *in vivo* function. *J. Biol. Chem.* **280,** 19437–19440 (2005).
10. Biskup, T. *et al.* Direct observation of a photoinduced radical pair in a cryptochrome blue-light photoreceptor. *Angew. Chem. Int. Ed.* **48,** 404–407 (2009).
11. Maeda, K. *et al.* Magnetically sensitive light-induced reactions in cryptochrome are consistent with its proposed role as a magnetoreceptor. *Proc. Natl Acad. Sci. USA* **109,** 4774–4779 (2012).
12. Niessner, C. *et al.* Magnetoreception: activated cryptochrome 1a concurs with magnetic orientation in birds. *J. R. Soc. Interface* **10,** 20130638 (2013).
13. Niessner, C., Denzau, S., Peichl, L., Wiltschko, W. & Wiltschko, R. Magnetoreception in birds: I. Immunohistochemical studies concerning the cryptochrome cycle. *J. Exp. Biol.* **217,** 4221–4224 (2014).
14. Lee, A. A. *et al.* Alternative radical pairs for cryptochrome-based magnetoreception. *J. R. Soc. Interface* **11,** 20131063 (2014).
15. Hogben, H. J., Efimova, O., Wagner-Rundell, N., Timmel, C. R. & Hore, P. J. Possible involvement of superoxide and dioxygen with cryptochrome in avian magnetoreception: origin of Zeeman resonances observed by *in vivo* EPR spectroscopy. *Chem. Phys. Lett.* **480,** 118–122 (2009).
16. Solov'yov, I. A. & Schulten, K. Magnetoreception through cryptochrome may involve superoxide. *Biophys. J.* **96,** 4804–4813 (2009).
17. Conrad, K. S., Manahan, C. C. & Crane, B. R. Photochemistry of flavoprotein light sensors. *Nature Chem. Biol.* **10,** 801–809 (2014).
18. Gao, J. *et al.* Trp triad-dependent rapid photoreduction is not required for the function of *Arabidopsis* CRY1. *Proc. Natl Acad. Sci. USA* **112,** 9135–9140 (2015).
19. Steiner, U. E. & Ulrich, T. Magnetic field effects in chemical kinetics and related phenomena. *Chem. Rev.* **89,** 51–147 (1989).
20. Liedvogel, M. & Mouritsen, H. Cryptochromes—a potential magnetoreceptor: what do we know and what do we want to know? *J. R. Soc. Interface* **7,** S147–S162 (2010).
21. Dodson, C. A., Hore, P. J. & Wallace, M. I. A radical sense of direction: signalling and mechanism in cryptochrome magnetoreception. *Trends Biochem. Sci.* **38,** 435–446 (2013).
22. Mouritsen, H. *et al.* Cryptochromes and neuronal-activity markers colocalize in the retina of migratory birds during magnetic orientation. *Proc. Natl Acad. Sci. USA* **101,** 14294–14299 (2004).
23. Möller, A., Sagasser, S., Wiltschko, W. & Schierwater, B. Retinal cryptochrome in a migratory passerine bird: a possible transducer for the avian magnetic compass. *Naturwissenschaften* **91,** 585–588 (2004).
24. Niessner, C. *et al.* Avian ultraviolet/violet cones identified as probable magnetoreceptors. *PLoS ONE* **6,** e20091 (2011).
25. Gegear, R. J., Casselman, A., Waddell, S. & Reppert, S. M. Cryptochrome mediates light-dependent magnetosensitivity in *Drosophila*. *Nature* **454,** 1014–1018 (2008).
26. Yoshii, T., Ahmad, M. & Helfrich-Forster, C. Cryptochrome mediates light-dependent magnetosensitivity of *Drosophila*'s circadian clock. *PLoS Biol.* **7,** 813–819 (2009).
27. Gegear, R. J., Foley, L. E., Casselman, A. & Reppert, S. M. Animal cryptochromes mediate magnetoreception by an unconventional photochemical mechanism. *Nature* **463,** 804–807 (2010).
28. Foley, L. E., Gegear, R. J. & Reppert, S. M. Human cryptochrome exhibits light-dependent magnetosensitivity. *Nature Commun.* **2,** 356 (2011).
29. Fedele, G. *et al.* Genetic analysis of circadian responses to low frequency electromagnetic fields in *Drosophila melanogaster*. *PLoS Genet.* **10,** e1004804 (2014).
30. Fedele, G., Green, E. W., Rosato, E. & Kyriacou, C. P. An electromagnetic field disrupts negative geotaxis in *Drosophila* via a CRY-dependent pathway. *Nature Commun.* **5,** 4391 (2014).
31. Marley, R., Giachello, C. N. G., Scrutton, N. S., Baines, R. A. & Jones, A. R. Cryptochrome-dependent magnetic field effect on seizure response in *Drosophila* larvae. *Sci. Rep.* **4,** 5799 (2014).
32. Ahmad, M., Galland, P., Ritz, T., Wiltschko, R. & Wiltschko, W. Magnetic intensity affects cryptochrome-dependent responses in *Arabidopsis thaliana*. *Planta* **225,** 615–624 (2007).
33. Harris, S.-R. *et al.* Effect of magnetic fields on cryptochrome-dependent responses in *Arabidopsis thaliana*. *J. R. Soc. Interface* **6,** 1193–1205 (2009).
34. Henbest, K. B. *et al.* Magnetic-field effect on the photoactivation reaction of *Escherichia coli* DNA photolyase. *Proc. Natl Acad. Sci. USA* **105,** 14395–14399 (2008).
35. Binhi, V. N. Stochastic dynamics of magnetosomes and a mechanism of biological orientation in the geomagnetic field. *Bioelectromagnetics* **27,** 58–63 (2006).
36. Winklhofer, M. & Kirschvink, J. L. A quantitative assessment of torque-transducer models for magnetoreception. *J. R. Soc. Interface* **7,** S273–S289 (2010).
37. Cai, J. Quantum probe and design for a chemical compass with magnetic nanostructures. *Phys. Rev. Lett.* **106,** 100501 (2011).
38. Miura, T., Maeda, K. & Arai, T. Effect of coulomb interaction on the dynamics of the radical pair in the system of flavin mononucleotide and hen egg-white lysozyme (HEWL) studied by a magnetic field effect. *J. Phys. Chem. B* **107,** 6474–6478 (2003).
39. Murakami, M., Maeda, K. & Arai, T. Dynamics of intramolecular electron transfer reaction of FAD studied by magnetic field effects on transient absorption spectra. *J. Phys. Chem. A* **109,** 5793–5800 (2005).
40. Neil, S. R. T. *et al.* Broadband cavity-enhanced detection of magnetic field effects in chemical models of a cryptochrome magnetoreceptor. *J. Phys. Chem. B* **118,** 4177–4184 (2014).
41. Evans, E. W. *et al.* Sensitive fluorescence-based detection of magnetic field effects in photoreactions of flavins. *Phys. Chem. Chem. Phys.* **17,** 18456–18463 (2015).
42. Dodson, C. A. *et al.* Fluorescence-detected magnetic field effects on radical pair reactions from femtolitre volumes. *Chem. Commun.* **51,** 8023–8026 (2015).

43. Beardmore, J. P., Antill, L. M. & Woodward, J. R. Optical absorption and magnetic field effect based imaging of transient radicals. *Angew. Chem.* **54,** 8494–8497 (2015).
44. Hore, P. J. & Broadhurst, R. W. Photo-CIDNP of biopolymers. *Prog. Nucl. Magn. Reson. Spectrosc.* **25,** 345–402 (1993).
45. Morozova, O. B. *et al.* Time resolved CIDNP study of electron transfer reactions in proteins and model compounds. *Mol. Phys.* **100,** 1187–1195 (2002).
46. Mok, K. H. & Hore, P. J. Photo-CIDNP NMR methods for studying protein folding. *Methods* **34,** 75–87 (2004).
47. Atkins, P. W. & Evans, G. T. Magnetic-field effects on chemiluminescent fluid solutions. *Mol. Phys.* **29,** 921–935 (1975).
48. Mani, T. & Vinogradov, S. A. Magnetic field effects on triplet–triplet annihilation in solutions: modulation of visible/NIR luminescence. *J. Phys. Chem. Lett.* **4,** 2799–2804 (2013).
49. Hore, P. J. & Kaptein, R. Proton nuclear magnetic-resonance assignments and surface accessibility of tryptophan residues in lysozyme using photochemically induced dynamic nuclear polarization spectroscopy. *Biochemistry* **22,** 1906–1911 (1983).
50. Vaish, S. P. & Tollin, G. Flash photolysis of flavins. V. Oxidation and disproportionation of flavin radicals. *J. Bioenerg.* **2,** 61–72 (1971).
51. Massey, V. Activation of molecular-oxygen by flavins and flavoproteins. *J. Biol. Chem.* **269,** 22459–22462 (1994).
52. Brocklehurst, B. Spin correlation in geminate recombination of radical ions in hydrocarbons. 1. Theory of magnetic-field effect. *J. Chem. Soc. Faraday Trans. II* **72,** 1869–1884 (1976).
53. Timmel, C. R., Till, U., Brocklehurst, B., McLauchlan, K. A. & Hore, P. J. Effects of weak magnetic fields on free radical recombination reactions. *Mol. Phys.* **95,** 71–89 (1998).
54. Weber, S. *et al.* Origin of light-induced spin-correlated radical pairs in cryptochrome. *J. Phys. Chem. B* **114,** 14745–14754 (2010).
55. Song, S. H. *et al.* Absorption and fluorescence spectroscopic characterization of cryptochrome 3 from *Arabidopsis thaliana*. *J. Photochem. Photobiol. B* **85,** 1–16 (2006).
56. Shirdel, J., Zirak, P., Penzkofer, A., Breitkreuz, H. & Wolf, E. Absorption and fluorescence spectroscopic characterisation of the circadian blue-light photoreceptor cryptochrome from *Drosophila melanogaster* (dCry). *Chem. Phys.* **352,** 35–47 (2008).
57. Weaver, J. C., Vaughan, T. E. & Astumian, R. D. Biological sensing of small field differences by magnetically sensitive chemical reactions. *Nature* **405,** 707–709 (2000).
58. Maeda, K. *et al.* Following radical pair reactions in solution: a step change in sensitivity using cavity ring-down detection. *J. Am. Chem. Soc.* **133,** 17807–17815 (2011).
59. Rodgers, C. T., Norman, S. A., Henbest, K. B., Timmel, C. R. & Hore, P. J. Determination of radical re-encounter probability distributions from magnetic field effects on reaction yields. *J. Am. Chem. Soc.* **129,** 6746–6755 (2007).
60. Hoang, N. *et al.* Human and *Drosophila* cryptochromes are light activated by flavin photoreduction in living cells. *PLoS Biol.* **6,** e160 (2008).
61. Bouly, J. P. *et al.* Cryptochrome blue light photoreceptors are activated through interconversion of flavin redox states. *J. Biol. Chem.* **282,** 9383–9391 (2007).

Acknowledgements

We thank N. Baker for expert technical assistance. E.W.E. is indebted to the Engineering and Physical Sciences Research Council and SABMiller plc for his doctoral scholarship. C. A.D. gratefully acknowledges her current Imperial College Junior Research Fellowship. We are grateful to the following for financial support: the Defense Advanced Research Projects Agency (QuBE: N66001-10-1-4061), the European Research Council (under the European Union's 7th Framework Programme, FP7/2007-2013/ERC grant agreement No. 340451), the Air Force Office of Scientific Research (Air Force Materiel Command, USAF award No. FA9550-14-1-0095) and the EMF Biological Research Trust.

Author contributions

D.R.K. and E.W.E. contributed equally to this work. D.R.K., E.W.E. and V.D. designed and performed the experiments. D.R.K. and E.W.E. analysed the data. C.A.D. advised on the production of the *At*Cry1 samples. M.I.W. helped oversee the fluorescence microscopy experiments. C.R.T., S.R.M. and P.J.H. coordinated the study. P.J.H., D.R.K. and E.W.E. wrote the paper. All the authors discussed the results and commented on the manuscript.

Additional information

Supplementary information is available in the online version of the paper. Reprints and permissions information is available online at www.nature.com/reprints. Correspondence and requests for materials should be addressed to P.J.H.

Competing financial interests

The authors declare no competing financial interests.